Title Page

Sildenafil does not prevent heart hypertrophy and fibrosis induced by cardiomyocyte AT_1R signaling

Julia Straubinger, Verena Schöttle, Nadja Bork, Hariharan Subramanian, Sarah Dünnes, Michael Russwurm, Meinrad Gawaz, Andreas Friebe, Mona Nemer, Viacheslav O. Nikolaev, Robert Lukowski

JS, VS, NB and RL: Department of Pharmacology, Toxicology and Clinical Pharmacy, Institute of Pharmacy, University of Tuebingen, Tuebingen, Germany

HS and VON: Institute of Experimental Cardiovascular Research, University Medical Center Hamburg-Eppendorf, Hamburg, Germany

SD and AF: Physiologisches Institut I, Universität Würzburg, Würzburg, Germany

MR: Institut für Pharmakologie und Toxikologie, Ruhr-Universität Bochum, Bochum, Germany

MG: Internal Medicine III, Cardiology and Cardiovascular Medicine, University Hospital Tuebingen, Tuebingen, Germany

MN: Laboratory of Cardiac Development and Differentiation, Department of Biochemistry, Microbiology, and Immunology, University of Ottawa, Ottawa, Ontario, Canada; and Institut de recherches cliniques de Montréal, Montréal, Québec, Canada

Running Title Page

Running Titel: SIL/cGMP and amplified AT_1R signaling in cardiomyocytes

Corresponding author: Robert Lukowski, Department of Pharmacology, Toxicology and Clinical Pharmacy, Institute of Pharmacy, University of Tübingen, Tel. +49 7071 29 74550, Fax +49 7071 29 2476, E-mail: robert.lukowski@uni-tuebingen.de

List of non-standard abbreviations: cGMP-dependent protein kinase type I (cGKI); protein kinase G (PKG); natriuretic peptides (NPs), cyclic guanosine-3´,5´-monophosphate (cGMP); nitric oxide (NO); cyclic adenosine-3´,5´-monophosphate (cAMP); Angiotensin II (AngII); Angiotensin II receptor type 1 (AT_1R); sildenafil (SIL); cardiomyocyte (CM), smooth muscle cell (SMC); angiotensin converting enzyme (ACE), cGKIβ rescue mice (βRM), phosphodiesterase (PDE); Förster resonance energy transfer (FRET); 3-isobutyl-1-methylxanthine (IBMX), C-type natriuretic peptide (CNP).

Section assignment: Cardiovascular

Number of words: 4141 (excluding abstract, material and methods, reference list and figure legends)

Number of words (abstract): 250

Number of references: 67

Page count: 37

Abstract

Analyses of several mouse models imply that the phosphodiesterase 5 (PDE5) inhibitor sildenafil (SIL), via increasing cyclic guanosine-3',5'-monophosphate (cGMP), affords protection against angiotensin II (AngII) stimulated cardiac remodeling. However, it is unclear which cell types are involved in these beneficial effects, because AngII may exert its adverse effects by modulating multiple reno-vascular and cardiac functions via AngII type 1 receptors (AT_1R). To test the hypothesis that SIL/cGMP oppose cardiac stress provoked by amplified AngII/AT_1R directly in cardiomyocytes (CMs), we studied transgenic mice with CM-specific overexpression of the AT_1R under the control of the α-myosin-heavy chain promoter (αMHC-$AT_1R^{tg/+}$). The extent of cardiac growth was assessed in absence or presence of SIL and defined by referring changes in heart-weight to body-weight or tibia length. Hypertrophic marker genes, extracellular matrix-regulating factors and expression patterns of fibrosis markers were examined in αMHC-$AT_1R^{tg/+}$ ventricles (±SIL) and corroborated by investigating different components of the natriuretic peptide (NP)/PDE5/cGMP pathway as well as cardiac functions. cGMP levels in heart lysates and intact CMs were measured by competitive immunoassays and FRET. We find higher cardiac and CM cGMP levels and up-regulation of the cGMP-dependent protein kinase I (cGKI) with AT_1R over-expression. However, even a prolonged SIL treatment regimen did not limit the progressive CM growth, fibrosis or decline in cardiac functions in the αMHC-$AT_1R^{tg/+}$ model suggesting that SIL does not interfere with the pathogenic actions of amplified AT_1R signaling in CMs. Hence, the cardiac/non-cardiac cells involved in the cross-talk between SIL-sensitive PDE activity and AngII/AT_1R need to be identified.

Introduction

Evidence from animal and clinical studies with angiotensin converting enzyme inhibitors (ACE) and antagonists of angiotensin II type 1 receptors (AT_1Rs) identified the AngII/AT_1 receptor pathway as a major cause for cardiac damage (de Gasparo et al., 2000; Lopez-Sendon et al., 2004; Higuchi et al., 2007; McMurray et al., 2012; Authors/Task Force et al., 2014). Kidney cross-transplantation experiments in gene-targeted mice suggest that selective ablation of renal AT_1Rs prevents adverse cardiac remodeling, whereas AT_1Rs in the heart are not involved in the AngII stimulated stress response *i.e.* pathological growth of cardiomyocytes (CMs) and fibrosis (Crowley et al., 2006). In contrast, different rodent models that overexpress the AT_1R in CMs reportedly developed hypertrophy, fibrosis, cardiac dysfunction (Paradis et al., 2000; Hoffmann et al., 2001; Ainscough et al., 2009) or premature death (Hein et al., 1997). Moreover, direct growth effects of AngII on cardiac fibroblasts and smooth-muscle cells (SMCs) (Griendling et al., 1997; Leask, 2010), and a strong interplay between the different kinds of cardiac cells are well-documented (Fredj et al., 2005; Kakkar and Lee, 2010; Takeda et al., 2010; Tirziu et al., 2010); hence interaction of AngII with responsive receptors at different cardio-vascular and renal locations may be important to elicit its pro-hypertrophic and pro-fibrotic effects.

The natriuretic peptide (NP)/cyclic guanosine-3',5'-monophosphate (cGMP) pathway has been shown to play an important cardio-protective role in the cardiac stress response stimulated by various factors including AngII (Li et al., 2002; Nishikimi et al., 2006; Kilic et al., 2007; Hofmann et al., 2009; Kinoshita et al., 2010; Bice et al., 2014). Interestingly, a combined strategy to prevent the degradation of several vasoactive peptides including the NPs and AT_1R blockade has recently given positive results in a large phase III clinical trial in patients with heart failure (McMurray et al., 2014). Among other modes of action, neprilysin inhibition is expected to increase the local bioavailability of endogenous NPs pointing to a role of the cGMP pathway in this setting. Along these lines, inhibition of the cGMP-hydrolyzing enzyme phosphodiesterase 5 (PDE5) using sildenafil (SIL) was shown to prevent or even reverse pressure overload-induced remodeling by transverse aortic constriction (TAC) in mice (Takimoto et al., 2005), showing beneficial effects in several other cardiac disease conditions such as ischemia/reperfusion injury and cardiotoxicity from doxorubicin (Kass, 2012). Based on these

findings, it has been suggested that favorable effects of SIL require cGMP and cGMP-dependent protein kinase type I (cGKI) in the CM (Takimoto et al., 2005; Takimoto et al., 2009; Koitabashi et al., 2010; Nishida et al., 2010), with the latter one being the major target of NP/cGMP signaling in the cardio-vascular system (Hofmann et al., 2009; Takimoto, 2012). Indeed, multiple targets downstream of NP or SIL and cGMP/cGKI were suggested to oppose adverse cardiac hypertrophy in response to AngII, elevated afterload and other causes (Tokudome et al., 2008; Takimoto et al., 2009; Klaiber et al., 2010; Koitabashi et al., 2010; Nishida et al., 2010; Frantz et al., 2013). However, analysis of a murine model that lacks the cGKIα and Iβ isoenzymes in all non-SMCs including the CMs (βRM), has challenged some of these previous findings (Lukowski et al., 2010). Cardiac growth responses to TAC or isoproterenol in βRM mice were normal suggesting that non-SMC cGKI is either not required to oppose pressure-overload and β-adrenergic receptor-triggered remodeling or cGMP/cGKI are not appropriately activated under these experimental conditions. Therefore, we previously applied a hypertensive dose of AngII and confirmed that anti-fibrotic effects of SIL (Westermann et al., 2012) were indeed related to non-SMC cGKI (Patrucco et al., 2014). The following points regarding the cellular targets of SIL/cGMP/cGKI and AngII are still open (Lukowski et al., 2014): i.) The vasoactive neuro-hormone AngII may provoke cardiac stress response by changes in hemodynamics *i.e.* an increase in afterload resulting from high blood pressure, and from direct effects on non-/CM cells. Therefore, changes in the fibrotic response upon AngII and SIL co-administration cannot easily be tracked down to a definite type of cell. ii.) SIL by itself may signal via different PDE5-expressing cells in the whole animal system, and iii.) SIL may affect the cardiac cGMP turn-over independently of PDE5 *e.g.* by an effect on PDE1C (Lukowski et al., 2010; Lukowski et al., 2014).

To this end, we studied mice that carry a CM-specific overexpression of the human AT_1R (αMHC-$AT_1R^{tg/+}$) (Paradis et al., 2000) to discriminate the cross-talk between SIL/cGMP and the AngII/AT_1R during adverse cardiac remodeling. Reportedly, AT_1R transgenic mice developed a severe cardiac phenotype *i.e.* progressive primary cardiomyocyte hypertrophy with secondary interstitial fibrosis in the absence of AngII (Yasuda et al., 2012) and high blood pressure (Paradis et al., 2000; Karnik and Unal, 2012). We tested whether SIL in a previously confirmed anti-fibrotic dose resulting in a free

plasma-concentration of 70 nM (Adamo et al., 2010; Patrucco et al., 2014) would interfere with amplified *in vivo* AT_1R signaling in the αMHC-$AT_1R^{tg/+}$ mouse model. Our data indicate that SIL does not prevent cardiac remodeling induced by CM-specific AT_1R overexpression, suggesting other cell types to be involved in the potentially favorable effects of this drug.

Methods

Animal welfare, ethical statements and genetic background of the experimental mice

Experimental mice were bred and maintained at the animal facility of the Institute of Pharmacy, Department of Pharmacology, Toxicology and Clinical Pharmacy, University of Tübingen. All procedures were performed with permission of the local authorities and conducted in accordance with the German legislation on the protection of animals. The mice were kept in temperature and humidity controlled cabinets, in cages with wood-chip bedding on a standard 12h light-dark cycles with ad libitum access to food (Altromin) and water. For experiments mice with a CM-restricted overexpression of the angiotensin II type 1 receptor (genotype: αMHC-$AT_1R^{tg/+}$) were compared to age- and litter-matched wild-type mice on a C57BL/6 genetic background (Paradis et al., 2000). Genotyping was performed by a previously established PCR protocol using mouse tail genomic DNA and a set of two primers (AT_1R forward: 5'- ACC CTT ACC CCA CAT AGA C -3'; AT_1R reverse: 5'- ACC ATC TTC AGT AGA AGA GTT G -3') that amplified the transgenic AT_1 allele (400 bp). Experimental mice were studied irrespective of their gender at an age of 8 to 24 weeks. For organ removal animals were sacrificed by CO_2 inhalation. All studies were performed in accordance with the ARRIVE guidelines for reporting experiments involving animals.

Long-term sildenafil application protocol

Previously assessed cardiac phenotypes of AT_1R transgenic mice upon 2 month of losartan treatment (30 mg/kg/day) revealed beneficial effects on various parameters of the adverse remodeling process (Paradis et al., 2000). Using an analogous protocol, sixty day-old AT_1R transgenic mice and control animals from the same litters received SIL (400 mg/l) in acidified drinking water (pH 4.5) water for 2 months. This dose of sildenafil was shown to be anti-fibrotic in an AngII-stimulated model of cardiac hypertrophy (Patrucco et al., 2014) and yielded an average plasma concentration of 70 nM (Adamo et al., 2010). This concentration is well in the range to inhibit the PDE5 (IC_{50}= 10 nM).

Transthoracic echocardiography

Non-invasive echocardiography was performed using an existing protocol with minor variations (Lukowski et al., 2010). In brief, high-resolution images were acquired by the use of an imaging systems equipped with a 30-MHz probe (Vevo 2100*;* VisualSonics, Toronto, Canada). Throughout the procedure mice were anaesthetised by a continuous oxygen/isoflurane (2%) inhalation. The chest was gently shaved and the area was cleaned with alcohol to minimize ultrasound reduction. For image acquisition mice were placed on a heated surgical platform in a dorsal position. From good quality 2D images obtained in the parasternal short-axis view, the fractional shortening (FS) and ejection fraction (EF) were assessed in M-mode recordings. Hemodynamic functions of the heart were calculated in three different positions from a total of nine independent measurements per mouse.

Isolation of adult cardiomyocytes from WT and αMHC-$AT_1R^{tg/+}$ hearts

Adult cardiomyocytes were isolated as described previously by a modified protocol of the Alliance for Cellular Signaling (AfCS, procedure protocol PP00000125) (Lukowski et al., 2010; Soltysinska et al., 2014). After retrograde enzyme perfusion via the aorta the hearts were minced into small pieces and myocytes were liberated by gently applying mechanical turbulence. For the quantification of the size b*y* planimetry using AxioVison Microscope Software 4.8 (Carl Zeiss) cells were plated in 6-well format and immediately photographed.

mRNA expression analysis using real-time quantitative PCR

Total RNA was purified from isolated heart ventricles with 500 µl peqGOLD RNA pure reagent (PEQLab Biotech.) according to the manufacturer´s protocol. The RNA concentration was assessed by UV photometry in a NanoPhotometer (Implen), and diluted in diethyl-pyrocarbonate treated ddH_2O to a final concentration of 0.1 µg/µl. 500 ng of the RNA was used as a template to synthesize cDNA using the iScript cDNA Synthesis Kit (Biorad). A 1:10 dilution of the cDNA was amplified using an iQ SYBR Green Supermix (Biorad) in an Opticon real-time quantitative PCR (qPCR) detections system (MJ Research) with specific primers. As consistent markers of heart hypertrophy or fibrosis the expression levels of atrial natriuretic peptide (ANP), brain natriuretic peptide (BNP), cardiac

sarcoplasmatic reticulum Ca^{2+}-ATPase-2 (SERCA2), myosin heavy chain alpha-isoform (MYHα), connective tissue growth factor (CTGF), alpha smooth muscle actin (α-SMA), collagen alpha-1 chain-1 (Col1A1), collagen alpha-1 chain-2 (Col1A2) matrix metalloprotease-9 (MMP9), and metallopeptidase inhibitor-1 (TIMP1) were determined and related to hypoxanthine-phosphoribosyl-transferase 1 (HPRT1) as an internal control for the qPCR reaction. The primer sequences designated were: ANP forward: 5'- TGT ACA GTG CGG TGT CCA AC -3'; ANP reverse: 5'- GGG GCA TGA CCT CAT CTT CT -3'; BNP forward: 5'- TCC TCT GGG AAG TCC TAG CC -3'; BNP reverse: 5'- GCC ATT TCC TCC GAC TTT TC -3'; SERCA2 forward: 5'- CTG CTG CAT GGT GGT TCA T -3'; SERCA2 reverse: 5'- TCC ACT CCA TCG AAG TCT GG -3'; αMHC forward: 5'- TGC TGA CAG ATC GGG AGA AT -3', αMHC reverse: 5'- TGC TGG CAA AGT ACT GGA TG -3'; CTGF forward: 5'- AGG GCC TCT TCT GCG ATT TC -3'; CTGF reverse: 5'-TAC ACC GAC CCA CCG AAG AC -3'; αSMA forward: 5'- AGA GGC ACC ACT GAA CCC TA -3'; αSMA reverse: 5'-GCA TAG AGG GAC AGC ACA GC -3'; Col1A1 forward: 5'- GAG GAA ACT TTG CTT CCC AGA -3'; Col1A1 reverse: 5'- ACC ACG AGG ACC AGA AGG AC -3'; Col1A2 forward: 5'- GTC TGT TGG AGC TGC TGG CCC AT -3'; Col1A2 reverse: 5'-GCA GCA CCA GGG AAG CCA GTC AT -3'; MMP9 forward: 5'- GGA GTT CTC TGG TGT GCC CT -3'; MMP9 reverse: 5'- ACA CGC CAG AAG AAT TTG CCA -3'; TIMP1 forward: 5'- CCA CCC ACA GAC AGC CTT CT -3', TIMP1 reverse: 5'- CGC TGG TAT AAG GTG GTC TCG -3'; HPRT1 forward: 5'- CAT TAT GCC GAG GAT TTG GA -3'; HPRT1 reverse: 5'- CCT TCA TGA CAT CTC GAG CA -3'. Additionally, we assessed the overexpression of the human Angiotensin 2 receptor type 1 (AT_1R) and the expression of the phosphodiesterases 5 (PDE5) using the following primer-pairs: AT_1R forward: 5'- ACA GTA TCA TCT TTG TGG TGG GA -3'; AT_1R reverse: 5'- GGC CAC AGT CTT CAG CTT CA -3'; PDE5 forward: 5'- GGA ACA CCA TCA TTT TGA CCA GT -3', PDE5 reverse: 5'-AGA GGC CAC TGA GAA TCT GGT -3'.

Immunoblotting of cardiac proteins

Western blot analysis was performed with protein extracts obtained from αMHC-$AT_1R^{tg/+}$ and control mice. Upon dissection and organ removal the residual blood in the heart chambers and vessels was

thoroughly removed via a retrograde injection of ice-cold phosphate-buffered saline (PBS) using a 1-ml syringe combined with a 25–gauge needle. Atria were immediately removed, and ventricles were frozen on liquid nitrogen, and stored at –80°C until homogenization was carried out for extraction of the total protein using lysis buffer (20 mM Tris-HCl, pH 8.3; 0.67% SDS; 238 mM β-mercaptoethanol; 0.2 mM PMSF). Proteins (50 µg/lane) were separated by their molecular weight using denaturing 10% SDS-PAGE. Immunodetection was performed by using the cGKI common antibody ((Methner et al., 2013); dilution 1:250), and a primary antibody specific for GAPDH (Cell Signaling; dilution 1:1000). To identify the primary antibody protein complexes a Cy5-coupled secondary anti-rabbit antibody (ECL Plex GE Healthcare; 1:2500 dilution) was used. Fluorophores were detected using the Ettan DIGE System (GE Healthcare).

Sirius Red, haematoxylin and eosin staining

For histology, hearts were dissected, rinsed in PBS, and fixed four hours in 2% paraformaldehyde (PFA) in PBS. Cryoprotection was accomplished by a series of sucrose solutions with increasing concentrations (5%, 10%, and 20%) in PBS. Neg-50 (Thermo Fisher Scientific) embedded organs were sectioned at 8-µm intervals (Microm HM 560 Cryostat, Thermo Scientific). Haematoxylin and eosin **(**H&E) staining were performed using standard procedures (Lukowski et al., 2010). The distribution and amount of extracellular collagen fibers was identified using a Sirius Red staining solution (Direct Red 80 in saturated picric acid) on sequential cardiac sections that were pre-treated for 24 h in Bouin's-fixative (5% acetic acid, 9% formaldehyde in saturated aqueous picric acid).

Measurement of cardiomyocyte size and fibrosis

Cardiomyocyte size was assessed in photomicrographs of H&E stained cross-sections using AxioVison Microscope Software 4.8 (Carl Zeiss). Cross-section areas of about 300-500 randomly chosen cells with a centrally located nucleus from n=9-12 hearts per genotype and treatment group were determined. For determining the amount of fibrosis Sirius Red stained sections were scanned using *MIRAX* Desk Scanner and illustrated with Mirax Viewer Software (Carl Zeiss). The GSA Image

Analyser software package was used for the quantification of red stained myocardial tissue and total ventricular areas.

cGMP determination in the heart and aorta.

For cGMP measurements, hearts from transgenic $AT_1R^{tg/+}$ mice that received either saline or sildenafil (400 mg/l) for 7 days were removed and flushed with ice-cold PBS. Further cGMP purification was performed as described earlier (Lukowski et al., 2008). In brief, the hearts were weighed before the cyclic nucleotides were extracted by homogenisation of the tissue using 1 ml ice-cold 100% EtOH. Resultant homogenates were centrifuged for 7 min at 13000 rpm. The supernatant containing the cyclic nucleotides was concentrated by evaporating the alcohol in a speed vac for 3-4 h at RT. The resulting pellet was resuspended in 115 µl EIA buffer. Cyclic GMP concentration in the samples was determined according to the manufacturer's recommendations of the EIA kit (Cayman chemical).

cGMP-PDE activity assay in heart cytosolic preparations

Whole hearts were homogenized in cold lysis buffer containing 50 mM NaCl, 1 mM EDTA, 2 mM DTT, 50 mM triethanolamine/HCl, pH 7.4, and protease inhibitors (1 µM pepstatin A, 1 mM benzamidine, 1 mM PMSF, and 50 µM leupeptin) using a glass-glass homogenizer. After centrifugation (30 min, 4 °C, 16,000 x g), PDE activity in the supernatant was measured by the conversion of ^{32P}-cGMP (synthesized from [α-^{32P}]GTP using purified guanylyl cyclase) to guanosine and ^{32P}-phosphate in the presence of alkaline phosphatase at 37 °C for 10 min. Reaction mixtures contained ^{32P}-cGMP (approx. 50,000 cpm), 1 µM cGMP, 12 mM $MgCl_2$, 3 mM DTT, 0.5 mg/ml BSA, 1 U of alkaline phosphatase, and 50 mM triethanolamine/HCl, pH 7.4, in a total volume of 0.1 ml. Reactions were stopped by the addition of 900 µl ice-cold charcoal suspension (30% activated charcoal in 50 mM KH_2PO_4, pH 2.3). After pelleting the charcoal by centrifugation, ^{32P}-phosphate was measured in the supernatant.

FRET-based cGMP measurements in intact cardiomyocytes.

To analyze CM-specific changes in cGMP levels, we crossed αMHC-$AT_1R^{tg/+}$ animals with red cGES-DE5 transgenic cGMP sensor mice (Gotz et al., 2014). Adult CMs were isolated from double-transgenic animals vs. littermate controls expressing the sensor without AT_1R overexpression and subjected to cGMP-FRET measurements under stimulation with C-type natriuretic peptide (CNP, 1 μM) and IBMX (100 μM) as previously described (Gotz et al., 2014).

Data analysis and statistical procedures

All values are expressed as mean ± SEM. Statistical significance was estimated by using Student's *t* test for unpaired observations with Excel software package (Fig. 1D, 2C-E, Fig. 3H-J, Supplemental Fig. 1C-F, Supplemental Fig. 1H-I, Supplemental Fig.. 2A-B). One-way ANOVA was used for comparison of more than two groups (Fig. 1B, Fig. 3A-F, Fig. 4B-F, Fig. 5B-D, Supplemental Fig. 1A) followed by a Turkey-Kramer Multiple Comparison post hoc test using GraphPad InStat 3.0. Statistical differences between genotypes and treatment conditions are indicated as p-values. Data were considered to be significant at $*^{/\#/\S}P < 0.05$, $**^{/\#\#/\S\S}P < 0.01$ and $***^{/\#\#\#/\S\S\S}P < 0.001$.

Results

Progressive heart hypertrophy and fibrosis in the αMHC-$AT_1R^{tg/+}$ mouse model

In order to re-validate the progressive cardiac phenotype of αMHC-$AT_1R^{tg/+}$ animals, cohorts of transgenic mice and wild-type (WT) age-matched littermates were sacrificed at different time-points after birth. Wet-weights of the dissected hearts (HW) were measured for every mouse and normalized either to the respective total body weight (BW) or the length of the tibia (TL) to determine HW/BW and HW/TL ratios (Supplemental Fig. 1A and data not shown). If anything we observed a decline in both ratios in WT animals with time, whereas the quantification of the αMHC-$AT_1R^{tg/+}$ ratios defined at 60, 120 and 160 days after birth showed a time-dependent increase of the HW/BW ratio from 5.55 ±0.05 mg/g to 6.04 ±0.19 mg/g and 6.48 ±0.33 mg/g, respectively (Supplemental Fig. 1A). Prominent increases in CM cross-section areas and in the dimensions of primary adult CMs as major causes for the abnormal growth of the hearts could be confirmed (Supplemental Fig. 1C and D) at AT_1R overexpression by >150-fold (Supplemental Fig. 1E) specifically in CMs (Supplemental Fig. 1F) (Paradis et al., 2000). Importantly, neither total body-weight nor any other body proportions including tibia lengths or naso-anal sizes were different between αMHC-$AT_1R^{tg/+}$ and WT litters (data not shown). In addition, the histopathology in the αMHC-$AT_1R^{tg/+}$ model was characterized by an extensive accumulation of extracellular matrix components (Supplemental Fig. 1G) and high transcript levels of genes associated with myocardial fibrosis, which both likely derived from activation of fibroblast-like cells secondary to chronic stimulation of AT_1R signal transduction in CMs (Supplemental Fig. 1G, H and I). These results are in good agreement with previous reports evaluating pathophysiological properties of the cardiac remodeling process in the αMHC-$AT_1R^{tg/+}$ mouse line (Paradis et al., 2000; Yasuda et al., 2012). As a potential cause underlying the cardiac phenotype of αMHC-$AT_1R^{tg/+}$ mice we considered a change in the relative balance between pro- and anti-hypertrophic factors in the CMs.

Cardiac cGMP/cGKI are stimulated upon AT_1R over-expression in CMs

We examined the potentially anti-hypertrophic and anti-fibrotic roles of cGMP signaling for the (AngII)/AT_1R-provoked defects in the CM (Booz, 2005) since an intensive cross-talk between these

pathways in different settings of cardiac stresses has been reported earlier (Li et al., 2002; Masuyama et al., 2006; Tokudome et al., 2008; Klaiber et al., 2010; Mokni et al., 2010; Frantz et al., 2013; Patrucco et al., 2014).

Using a genetically encoded cGMP FRET-based sensor in intact adult CMs (Gotz et al., 2014), we observed that CNP induced a ~2-fold higher cGMP elevation in $AT_1R^{tg/+}$ cells (isolated from 120-day old double transgenic mice) compared to control mice that only carried the FRET-based sensor (Figure 1A). However, IBMX following CNP treatment attenuated this difference in cGMP between the two genotypes (Figure 1B). Interestingly, IBMX alone increased the basal cGMP level only in control CMs with a much less pronounced effect in double transgenic mouse cells, suggesting a reduction of PDE-mediated effects on cGMP in $AT_1R^{tg/+}$ CMs under these experimental conditions (Figure 1C, D). By using validated cGKI common specific antibodies (Geiselhoringer et al., 2004) we identified higher abundance of cardiac cGKI in protein lysates derived from 120 and 160 days-old αMHC-$AT_1R^{tg/+}$ hearts as compared to WT samples (Figure 2A-D). In addition to cGKI, basal cGMP concentrations measured in αMHC-$AT_1R^{tg/+}$ whole heart lysates were increased (Figure 2E) confirming activation of the cGMP/cGKI pathway in a setting of amplified AngII/AT_1R in CMs.

Based on these findings, we reasoned that long-term stimulation of cGMP signaling in CMs may ameliorate the cardiac phenotype *i.e.* detrimental changes in heart dimension and structure of αMHC-$AT_1R^{tg/+}$ mice. In order to test whether PDE5-sensitive cGMP pools are involved in the protection against amplified AT_1R signaling, SIL was administered *ad libitum* via the drinking water at a concentration of 400 mg/l. We treated αMHC-$AT_1R^{tg/+}$ and WT mice for 60 consecutive days and evaluated the effects of SIL on different histological and functional parameters in comparison to two cohorts of age-matched littermates from both genotypes that served as untreated controls, respectively (Figure 2F and G). An analogous long-term SIL regimen previously resulted in an average plasma level of about 70 nM (Adamo et al., 2010); hence the drug concentration should be well above the IC_{50} value to inhibit the PDE5 and about 7-fold higher than the levels required for the inhibition of TAC-induced cardiac remodeling (Takimoto et al., 2005).

SIL does not counteract the progressive cardiac stress phenotype in αMHC-$AT_1R^{tg/+}$ mice

Long-term SIL administration neither affected the body-weight gain nor the survival rates of αMHC-$AT_1R^{tg/+}$ or WT mice (data not shown). Cardiac remodeling was evaluated at the end of the treatment period in 120 days-old WT and αMHC-$AT_1R^{tg/+}$ animals (Figure 3). Quantifications of gross parameters such as the HW/BW and HW/TL ratios did not reveal any beneficial effects of SIL on the extent of heart growth in the αMHC-$AT_1R^{tg/+}$ model (Figure 3A and B). To exclude the possibility that the $AT_1R^{tg/+}$ overexpression induced early alterations in myocardial structure which were not reversible at 60 days of age (or later), an additional group of αMHC-$AT_1R^{tg/+}$ animals received SIL for 80 days shortly after weaning *i.e.* at 40 days of age. As compared to the respective 60 days SIL treatment group, the prolonged protocol did not show a significant effect on the HW/BW and HW/TL ratios at 120 days of age (Supplemental Fig. 2A+B). We further evaluated the expression levels of hypertrophic marker genes such as atrial and brain natriuretic peptides (ANP and BNP), αMHC and SERCA2 (Figure 3C-F). As compared to WT hearts, the mRNA levels for ANP and BNP in αMHC-$AT_1R^{tg/+}$ hearts were about 4-10 fold higher under both control and SIL treated conditions (Figure 3C and D) supporting that the NP/cGMP/cGKI pathway is activated in response to amplified AT_1R signaling in CMs. However, neither the mRNA level of the hypertrophic markers ANP and BNP (Figure 3C and D) nor the amount of αMHC and SERCA2 mRNA (Figure 3E and F) or the expression level of the human AT_1R itself (data not shown) in the αMHC-$AT_1R^{tg/+}$ model were affected/sensitive by/to the long-term SIL protocol. If anything, the significant difference in SERCA2 mRNA levels between untreated WT and MHC-$AT_1R^{tg/+}$ mice was less pronounced in the presence of SIL (Fig. 3F). Our quantifications of different hypertrophy markers were in excellent agreement with histo-morphological examinations of the CM dimensions (Figure 3G and H). Importantly, the mean size of the CMs from αMHC-$AT_1R^{tg/+}$ mice that either received SIL or remained untreated was identical (Figure 3G and H). Since CM-specific defects *i.e.* the maladaptive hypertrophic growth in the αMHC-$AT_1R^{tg/+}$ mouse model was not opposed by SIL, we conclude that the rise in both global cardiac and aortic cGMP concentrations as measured at day 7 of the SIL treatment (Figure 3I and J) had no impact on the CMs.

Several recent reports suggested an anti-fibrotic mode of action for SIL and cGMP/cGKI on the cardiac stress response caused by AngII infusions (Westermann et al., 2012; Patrucco et al., 2014). We tested the effect of long-term SIL on the fibrotic response in the absence of high AngII, but with amplified AT_1R signaling in CMs. We determined the amount of interstitial extracellular matrix (ECM) proteins *i.e.* collagens. Cardiac tissue samples from ±SIL treated αMHC-$AT_1R^{tg/+}$ mice were examined from 120 days old animals (Figure 4A and B). Histologically, pronounced fibrosis of the papillary muscle and myocardium was apparent in αMHC-$AT_1R^{tg/+}$ hearts obtained from both control and SIL treated groups. As expected, the amount of ECM proteins and the levels of the fibrosis markers were in general lower in WT as compared to αMHC-$AT_1R^{tg/+}$ heart sections (Figure 4). To further asses the fibrotic response in the two αMHC-$AT_1R^{tg/+}$ treatment groups, we quantified the transcription levels of several genes associated with extracellular matrix (ECM) turn-over and fibrosis including Col1A1, Col1A2 (Fig. 4C-D), MMP9 and TIMP1 (Figure 4E-F). In line with the histological quantifications (Figure 4B), SIL did not affect the transcription levels of the pro-fibrotic genes Col1A1, Col1A2, whereas the differences in TIMP1 and MMP9 mRNA between the SIL treated WT and αMHC-$AT_1R^{tg/+}$ hearts reached the significance level (compare section sign (§) groups in Fig. 4E-F). However, a similar tendency to different turnover rates of the ECM components was also observed in the untreated WT *versus* αMHC-$AT_1R^{tg/+}$ groups (Fig. 4C-F) confirming that SIL did not affect the total amount of fibrosis deposition upon overexpression of the human AT_1R in CMs.

Amplified AT_1R signaling in the CM reportedly caused a gradual decline in cardiac functions (Paradis et al., 2000; Hoffmann et al., 2001; Yasuda et al., 2012), whereas SIL afforded cardio-protection and improved heart pump functions in different settings of cardiac stress (Takimoto et al., 2005; Takimoto et al., 2009; Adamo et al., 2010; Zhang et al., 2010; Blanton et al., 2012; Westermann et al., 2012). Hence, we assessed a number of echocardiographic parameters in anesthetized 120 days old WT and αMHC-$AT_1R^{tg/+}$ mice that received either SIL or placebo for 60 days (Figure 5A1 and A2). In agreement with previous studies (Rivard et al., 2011; Yasuda et al., 2012), the contractility of the heart muscle and the cardiac ejection fraction were severely disturbed in αMHC-$AT_1R^{tg/+}$ mice (Figure 5B and C) but these parameters were not altered by SIL (Figure 5B and C). Moreover, the cardiac PDE5 mRNA expression (Figure 5D) remained stable over time and did not differ between the two

genotypes. Due to this outcome, we reasoned that the inability of SIL to affect function and growth parameters of αMHC-$AT_1R^{tg/+}$ hearts was not caused by an unexpected regulation of its primary drug target.

The cGMP-hydrolytic activity of αMHC-$AT_1R^{tg/+}$ heart lysates in response to SIL

SIL at concentrations that should specifically inhibit PDE5 (≤ 10 nM) had no effect on the cGMP-hydrolytic activity in WT or hypertrophic αMHC-$AT_1R^{tg/+}$ heart lysates (Figure 5E and F). With excessive amounts of SIL (100-1000 nM), however, a moderate but reproducible inhibition of the cardiac cGMP hydrolytic activity was observed in both genotypes indicating inhibition of cardiac cGMP-PDEs different from PDE5 (Lukowski et al., 2014). When total heart PDE activity was determined in the presence of Ca^{2+}/calmodulin we observed a similar left shift of the inhibitory curves in both genotypes (Figure 5E and F) suggesting involvement of cardiac PDE1C. Under these experimental conditions (Figure 5F), SIL could significantly suppress the cGMP-hydrolyzing activity in the murine hearts only at relatively high concentrations (IC_{50} >1000 nM) which were likely not reached by the *in vivo* drug application protocol used herein (Adamo et al., 2010).

Together, the current data allow us to conclude that in the presence of amplified AT_1R signal transduction in murine CMs and hypertrophic heart disease, potentially beneficial effects of cGMP do not involve SIL/PDE5 directly in these cells (Lukowski et al., 2010; Mokni et al., 2010; Lukowski et al., 2014; Degen et al., 2015).

Discussion

Herein, we studied normotone transgenic mice that develop myocyte hypertrophy and fibrosis as a result of chronic AT_1R overexpression specifically in CMs (Paradis et al., 2000). At baseline, $AT_1R^{tg/+}$ hearts exhibited high expression of ANP and BNP (Figure 3) as well as increased levels of cGMP and cGKI (Figure 2) suggesting an activated NP/cGMP pathway. This was further supported by our finding that CNP induce a higher cGMP level in $AT_1R^{tg/+}$ compared to control CMs (Figure 1). Activation of the NP/cGMP pathway has been widely recognized in different cardiac stress models and is usually thought to be part of a counter-regulatory mechanism suppressing $G\alpha_q$–dependent Ca^{2+} signaling (Nishikimi et al., 2006; Kilic et al., 2007; Tokudome et al., 2008; Takimoto et al., 2009; Kinoshita et al., 2010; Klaiber et al., 2010; Koitabashi et al., 2010; Nishida et al., 2010; Frantz et al., 2013). As expected from previous studies (Adamo et al., 2010; Patrucco et al., 2014), SIL supplemented at high concentrations in drinking water stimulated cGMP levels in the cardio-vascular system (Figure 3I and J). However, this drug did not affect adverse remodeling processes, expression patterns of hypertrophic and fibrotic marker genes (Figure 3 and 4) or the contractility of the heart muscle in the αMHC-$AT_1R^{tg/+}$ mouse model (Figure 5). Based on these findings, we conclude that PDE5/cGMP does not interfere with amplified AngII/AT_1R signaling in the CM itself, hence the reported cardio-protective effects of PDE5 inhibition should occur in cells distinct from CMs. Recently, a SIL co-administration regimen was shown to prevent functional decline and adverse remodeling of AngII-stimulated hypertensive hearts (Westermann et al., 2012). This study did not differentiate between distinct cells types and systems that express the AT_1R and may benefit from the SIL treatment. However, these findings support the concept of a common cardio-protective SIL/PDE5/cGMP pathway in non-myocytes (Lukowski et al., 2014). It seems unlikely that the blood pressure and afterload lowering effects of SIL caused by the drug-induced changes in vascular tone are significant modulators of cardiac remodeling, since a corresponding anti-hypertensive treatment with hydralazine did not exhibit any signs of protection against the AngII-induced cardiac fibrosis and hypertrophy (Westermann et al., 2012). We detected a small but significant effect of long-term SIL on the turn-over of the ECM components in MHC-$AT_1R^{tg/+}$ hearts (compare section sign (§) groups in Figure 4C-F). The implication of this finding and its therapeutic relevance is unclear, in particular

because i.) untreated MHC-$AT_1R^{tg/+}$ hearts in our study showed a similar overall tendency (Figure 4C-F) and ii.) SIL did not affect any other parameter of the fibrotic response upon selective overexpression of the $AT_1R^{tg/+}$ in the CMs. Yet, we take this evidence as a rather consistent indicator for the anti-fibrotic actions attributed to SIL in different rodent models of adverse cardiac remodeling (Table 1).

The presented results from the αMHC-$AT_1R^{tg/+}$ model seem to be in contrast to some of the previous reports suggesting a cardio-protective role for SIL/PDE5 in pre-clinical models of TAC- (Takimoto et al., 2005; Nagayama et al., 2009; Takimoto et al., 2009; Blanton et al., 2012), post-MI- (Ockaili et al., 2002; Salloum et al., 2008) and pulmonary hypertension-induced remodeling and dysfunction (Xie et al., 2012). However, not all aspects of the SIL-dependent cardio-protection were reproduced in other studies (Andersen et al., 2008; Schafer et al., 2009; Kukreja et al., 2014; Lee et al., 2015). It is important to note that in the current study, we assessed the role of SIL for primary defects arising specifically in CMs in the absence of neuro-hormonal changes and elevated blood pressure.

So far, the cell types in which SIL interferes with AngII/AT_1R induced cardiac remodeling still remain elusive. Exposure of gene-targeted mice that lack cGKI in all non-SMCs with a pressure-dose of AngII demonstrated anti-fibrotic rather than anti-hypertrophic modes of action for SIL/PDE5/cGMP/cGKI signaling (Patrucco et al., 2014). It seems reasonable that cardiac fibroblasts are the primary target of SIL since they display the full repertoire for the cross-talk between PDE5/cGMP/cGKI and AT_1R, and the presence of PDE5 in murine CMs (Lukowski et al., 2010) and heart (Degen et al., 2015) was recently challenged. Increased cardiac and aortic cGMP concentrations in the presence of SIL (Figure 3) suggest that the cGMP system in the αMHC-$AT_1R^{tg/+}$ model is not fully activated; hence cGMP-elevating compounds which do not act directly on PDE5 may still elicit cardio-protection upon AT_1R overexpression. Because short-term SIL efficiently raised both the global cardiac and aortic cGMP levels, we find it very unlikely that the overexpression of AT_1R *per se* can change signaling pathways (*e.g.* NO-dependent cGMP production) that render the drug inactive (Lee et al., 2015). However, we cannot rule out that the rather large increase in AT_1R expression levels in CMs (Supplemental Fig. 1E and F) overrides the potentially beneficial effects of SIL by a yet unknown mechanism *in vivo*, whereas directly blocking AT_1Rs with losartan still prevented the

progressive remodelling processes with cardiac dysfunctions in αMHC-$AT_1R^{tg/+}$ mice (Paradis et al., 2000).

For the conditions tested, our global heart cGMP-PDE assay did not reveal any statistical differences in the cGMP hydrolyzing activity between αMHC-$AT_1R^{tg/+}$ and WT hearts (Figure 5E and F). However, we observed baseline elevation of cGMP/cGKI (Figure 1 and 2) as well as a reliable increase in the cardiac cGMP levels upon 7 days of SIL in αMHC-$AT_1R^{tg/+}$ mice (Fig. 2E). Apparently, it requires up-stream factors such as NO and/or the NPs and intact cellular compartments in order to stimulate the cardiac cGMP system via SIL-sensitive PDEs. Because our FRET sensor does not allow reliable measurements of the basal cGMP in CMs, the cGMP-PDE activity under these conditions *i.e.* in the absence of exogenous factors that activate the cGMP system, remains elusive (Figure 1A and C). However, our single-cell cGMP recordings under combined application of CNP plus IBMX (Figure 1B) and of IBMX alone (Figure 1D) suggest a dynamic regulation of the PDE-mediated effects on the NP/cGMP pathway upon a prolonged AT_1R overexpression in CMs. As IBMX is an unspecific PDE inhibitor, it was not possible to identify the isoform responsible for the changes in the cGMP-PDE response seen in intact CMs. Future studies will need to test the role of other PDEs, including the recently identified IBMX-insensitive cGMP-PDE9 (Keravis and Lugnier, 2012) in CMs (Lee et al., 2015) for the progressive heart phenotype in the αMHC-$AT_1R^{tg/+}$ model.

Although we were unable to detect much of the cGMP-hydrolyzing PDE5 activity in total heart lysates (Figure 5E and F), the Ca^{2+}/calmodulin sensitivity of the total heart lysates confirmed that cGMP-PDEs of the Ca^{2+}/calmodulin-dependent PDE1 family contribute to the global cGMP-hydrolyzing activity in the healthy and hypertrophic murine heart (Lukowski et al., 2010). In particular, PDE1C may have a role in the integration of cGMP and cAMP signaling because this PDE hydrolyzes both second messengers with similar catalytic rates (Vandeput et al., 2007). Pharmacological inhibition of PDE1 activity significantly reduced cardiac hypertrophy in the isoproterenol-induced mouse model of hypertrophy (Miller et al., 2009) establishing a critical role for CM PDE1 *in vivo*. In AngII-infused

rats PDE1, but not PDE5 activation reduced arterial cGMP bioavailability and increased contractile responsiveness (Giachini et al., 2011) suggesting a possible link between AngII/AT_1R and PDE1 signaling. To the best of our knowledge, the role of PDE1C has not been tested so far in an animal model of heart hypertrophy caused by AngII infusion.

In summary, the results of our study show that the AT_1R-induced pro-fibrotic and pro-hypertrophic signal transduction in CMs is not sensitive to PDE5 inhibition by SIL. Taking into account recent in-human trials demonstrating clinical failure of SIL treatment in heart failure with preserved ejection fraction (Redfield et al., 2013) and diastolic dysfunction after myocardial infarction (Andersen et al., 2013), we believe it might be important to reassess the cell type-specific consequences of PDE5 inhibition in suitable pre-clinical models of cardiac stress *i.e.* in mice that lack PDE5, PDE1C and/or cGKI specifically in cardiac myocytes and in other cardiovascular cell types. In a clinical setting, the final outcome is certainly one of the most important issues of a drug treatment. If the mechanisms of SIL action in animal models include several cell types, this could well influence the efficacy and side effects of the treatment and how human clinical trials should be set up. From the scientific point of view, it is also important to define the actual molecular targets (and target cells) of SIL *in vivo* since only such studies can provide detailed insight into the role of e.g. cGMP, SIL-sensitive PDEs (or other, potentially not yet identified molecules) for the pathomechanism(s) of hypertrophic heart disease. This year marks more than ten years of pre-clinical studies regarding the effects of SIL on the cardiac PDE5/cGMP/cGKI pathway (s. Table 1 for an overview). Based on what we have learned so far, it seems reasonable to conclude that the potential of SIL to oppose hypertrophic growth changes that develop at the bottom of a number of cardio-vascular diseases may turn out to be rather limited.

Acknowledgements

The authors thank Tanja Schönberger, Michael Glaser and Katrin Junger for excellent technical help and Franz Hofmann (FOR923, Institut für Pharmakologie und Toxikologie, Technische Unversität München) and Peter Ruth (Department of Pharmacology, Toxicology and Clinical Pharmacy, Institute of Pharmacy, University of Tuebingen, Tuebingen, Germany) for helpful discussions.

Authorship contributions

Participated in research design: RL, AF and VON.

Conducted experiments: JS, VS, NB, SD and HS.

Contributed new reagents or analytic tools: MG, MN and MR.

Performed data analysis: JS, VS, NB, SD, HS, AF, VON and RL.

Wrote or contributed to the writing of the manuscript: RL, AF and VON.

References

Adamo CM, Dai DF, Percival JM, Minami E, Willis MS, Patrucco E, Froehner SC and Beavo JA (2010) Sildenafil reverses cardiac dysfunction in the mdx mouse model of Duchenne muscular dystrophy. *Proceedings of the National Academy of Sciences of the United States of America* **107**:19079-19083.

Ainscough JF, Drinkhill MJ, Sedo A, Turner NA, Brooke DA, Balmforth AJ and Ball SG (2009) Angiotensin II type-1 receptor activation in the adult heart causes blood pressure-independent hypertrophy and cardiac dysfunction. *Cardiovascular research* **81**:592-600.

Andersen A, Nielsen JM, Peters CD, Schou UK, Sloth E and Nielsen-Kudsk JE (2008) Effects of phosphodiesterase-5 inhibition by sildenafil in the pressure overloaded right heart. *European journal of heart failure* **10**:1158-1165.

Andersen MJ, Ersboll M, Axelsson A, Gustafsson F, Hassager C, Kober L, Borlaug BA, Boesgaard S, Skovgaard LT and Moller JE (2013) Sildenafil and diastolic dysfunction after acute myocardial infarction in patients with preserved ejection fraction: the Sildenafil and Diastolic Dysfunction After Acute Myocardial Infarction (SIDAMI) trial. *Circulation* **127**:1200-1208.

Authors/Task Force m, Elliott PM, Anastasakis A, Borger MA, Borggrefe M, Cecchi F, Charron P, Hagege AA, Lafont A, Limongelli G, Mahrholdt H, McKenna WJ, Mogensen J, Nihoyannopoulos P, Nistri S, Pieper PG, Pieske B, Rapezzi C, Rutten FH, Tillmanns C, Watkins H and Authors/Task Force m (2014) 2014 ESC Guidelines on diagnosis and management of hypertrophic cardiomyopathy: The Task Force for the Diagnosis and Management of Hypertrophic Cardiomyopathy of the European Society of Cardiology (ESC). *European heart journal*.

Bice JS, Burley DS and Baxter GF (2014) Novel approaches and opportunities for cardioprotective signaling through 3',5'-cyclic guanosine monophosphate manipulation. *Journal of cardiovascular pharmacology and therapeutics* **19**:269-282.

Blanton RM, Takimoto E, Lane AM, Aronovitz M, Piotrowski R, Karas RH, Kass DA and Mendelsohn ME (2012) Protein kinase g ialpha inhibits pressure overload-induced cardiac

remodeling and is required for the cardioprotective effect of sildenafil in vivo. *Journal of the American Heart Association* **1**:e003731.

Booz GW (2005) Putting the brakes on cardiac hypertrophy: exploiting the NO-cGMP counter-regulatory system. *Hypertension* **45**:341-346.

Borgdorff MA, Bartelds B, Dickinson MG, van Wiechen MP, Steendijk P, de Vroomen M and Berger RM (2014) Sildenafil treatment in established right ventricular dysfunction improves diastolic function and attenuates interstitial fibrosis independent from afterload. *American journal of physiology Heart and circulatory physiology* **307**:H361-369.

Crowley SD, Gurley SB, Herrera MJ, Ruiz P, Griffiths R, Kumar AP, Kim HS, Smithies O, Le TH and Coffman TM (2006) Angiotensin II causes hypertension and cardiac hypertrophy through its receptors in the kidney. *Proceedings of the National Academy of Sciences of the United States of America* **103**:17985-17990.

de Gasparo M, Catt KJ, Inagami T, Wright JW and Unger T (2000) International union of pharmacology. XXIII. The angiotensin II receptors. *Pharmacological reviews* **52**:415-472.

Degen CV, Bishu K, Zakeri R, Ogut O, Redfield MM and Brozovich FV (2015) The Emperor's New Clothes: PDE5 and the Heart. *PloS one* **10**:e0118664.

Frantz S, Klaiber M, Baba HA, Oberwinkler H, Volker K, Gabetaner B, Bayer B, Abebetaer M, Schuh K, Feil R, Hofmann F and Kuhn M (2013) Stress-dependent dilated cardiomyopathy in mice with cardiomyocyte-restricted inactivation of cyclic GMP-dependent protein kinase I. *European heart journal* **34**:1233-1244.

Fredj S, Bescond J, Louault C and Potreau D (2005) Interactions between cardiac cells enhance cardiomyocyte hypertrophy and increase fibroblast proliferation. *Journal of cellular physiology* **202**:891-899.

Geiselhoringer A, Gaisa M, Hofmann F and Schlossmann J (2004) Distribution of IRAG and cGKI-isoforms in murine tissues. *FEBS letters* **575**:19-22.

Giachini FR, Lima VV, Carneiro FS, Tostes RC and Webb RC (2011) Decreased cGMP level contributes to increased contraction in arteries from hypertensive rats: role of phosphodiesterase 1. *Hypertension* **57**:655-663.

Gotz KR, Sprenger JU, Perera RK, Steinbrecher JH, Lehnart SE, Kuhn M, Gorelik J, Balligand JL and Nikolaev VO (2014) Transgenic mice for real-time visualization of cGMP in intact adult cardiomyocytes. *Circulation research* **114**:1235-1245.

Griendling KK, Ushio-Fukai M, Lassegue B and Alexander RW (1997) Angiotensin II signaling in vascular smooth muscle. New concepts. *Hypertension* **29**:366-373.

Hein L, Stevens ME, Barsh GS, Pratt RE, Kobilka BK and Dzau VJ (1997) Overexpression of angiotensin AT1 receptor transgene in the mouse myocardium produces a lethal phenotype associated with myocyte hyperplasia and heart block. *Proceedings of the National Academy of Sciences of the United States of America* **94**:6391-6396.

Higuchi S, Ohtsu H, Suzuki H, Shirai H, Frank GD and Eguchi S (2007) Angiotensin II signal transduction through the AT1 receptor: novel insights into mechanisms and pathophysiology. *Clin Sci (Lond)* **112**:417-428.

Hoffmann S, Krause T, van Geel PP, Willenbrock R, Pagel I, Pinto YM, Buikema H, van Gilst WH, Lindschau C, Paul M, Inagami T, Ganten D and Urata H (2001) Overexpression of the human angiotensin II type 1 receptor in the rat heart augments load induced cardiac hypertrophy. *J Mol Med (Berl)* **79**:601-608.

Hofmann F, Bernhard D, Lukowski R and Weinmeister P (2009) cGMP regulated protein kinases (cGK). *Handbook of experimental pharmacology*:137-162.

Kakkar R and Lee RT (2010) Intramyocardial fibroblast myocyte communication. *Circulation research* **106**:47-57.

Karnik SS and Unal H (2012) Angiotensin II receptor-induced cardiac remodeling in mice without angiotensin II. *Hypertension* **59**:542-544.

Kass DA (2012) Cardiac role of cyclic-GMP hydrolyzing phosphodiesterase type 5: from experimental models to clinical trials. *Current heart failure reports* **9**:192-199.

Keravis T and Lugnier C (2012) Cyclic nucleotide phosphodiesterase (PDE) isozymes as targets of the intracellular signalling network: benefits of PDE inhibitors in various diseases and perspectives for future therapeutic developments. *British journal of pharmacology* **165**:1288-1305.

Kilic A, Bubikat A, Gassner B, Baba HA and Kuhn M (2007) Local actions of atrial natriuretic peptide counteract angiotensin II stimulated cardiac remodeling. *Endocrinology* **148**:4162-4169.

Kinoshita H, Kuwahara K, Nishida M, Jian Z, Rong X, Kiyonaka S, Kuwabara Y, Kurose H, Inoue R, Mori Y, Li Y, Nakagawa Y, Usami S, Fujiwara M, Yamada Y, Minami T, Ueshima K and Nakao K (2010) Inhibition of TRPC6 channel activity contributes to the antihypertrophic effects of natriuretic peptides-guanylyl cyclase-A signaling in the heart. *Circulation research* **106**:1849-1860.

Klaiber M, Kruse M, Volker K, Schroter J, Feil R, Freichel M, Gerling A, Feil S, Dietrich A, Londono JE, Baba HA, Abramowitz J, Birnbaumer L, Penninger JM, Pongs O and Kuhn M (2010) Novel insights into the mechanisms mediating the local antihypertrophic effects of cardiac atrial natriuretic peptide: role of cGMP-dependent protein kinase and RGS2. *Basic research in cardiology* **105**:583-595.

Koitabashi N, Aiba T, Hesketh GG, Rowell J, Zhang M, Takimoto E, Tomaselli GF and Kass DA (2010) Cyclic GMP/PKG-dependent inhibition of TRPC6 channel activity and expression negatively regulates cardiomyocyte NFAT activation Novel mechanism of cardiac stress modulation by PDE5 inhibition. *Journal of molecular and cellular cardiology* **48**:713-724.

Kukreja R, Tang X-L, Lefer D, Steenbergen C, Jones S, Guo Y, Li Q, Kong M, Stowers H, Hunt G, Tokita Y, Wu W, Ockaili R, Salloum F, Book M, Du J, Bhushan S, Goodchild T, Chang C and Bolli R (2014) Administration of Sildenafil at Reperfusion Fails to Reduce Infarct Size: Results from the CAESAR Cardioprotection Consortium (LB650). *The FASEB Journal* **28**.

Leask A (2010) Potential therapeutic targets for cardiac fibrosis: TGFbeta, angiotensin, endothelin, CCN2, and PDGF, partners in fibroblast activation. *Circulation research* **106**:1675-1680.

Lee DI, Zhu G, Sasaki T, Cho GS, Hamdani N, Holewinski R, Jo SH, Danner T, Zhang M, Rainer PP, Bedja D, Kirk JA, Ranek MJ, Dostmann WR, Kwon C, Margulies KB, Van Eyk JE, Paulus WJ, Takimoto E and Kass DA (2015) Phosphodiesterase 9A controls nitric-oxide-independent cGMP and hypertrophic heart disease. *Nature* **519**:472-476.

Li Y, Kishimoto I, Saito Y, Harada M, Kuwahara K, Izumi T, Takahashi N, Kawakami R, Tanimoto K, Nakagawa Y, Nakanishi M, Adachi Y, Garbers DL, Fukamizu A and Nakao K (2002) Guanylyl cyclase-A inhibits angiotensin II type 1A receptor-mediated cardiac remodeling, an endogenous protective mechanism in the heart. *Circulation* **106**:1722-1728.

Lopez-Sendon J, Swedberg K, McMurray J, Tamargo J, Maggioni AP, Dargie H, Tendera M, Waagstein F, Kjekshus J, Lechat P, Torp-Pedersen C and Task Force on ACEiotESoC (2004) Expert consensus document on angiotensin converting enzyme inhibitors in cardiovascular disease. The Task Force on ACE-inhibitors of the European Society of Cardiology. *European heart journal* **25**:1454-1470.

Lukowski R, Krieg T, Rybalkin SD, Beavo J and Hofmann F (2014) Turning on cGMP-dependent pathways to treat cardiac dysfunctions: boom, bust, and beyond. *Trends in pharmacological sciences* **35**:404-413.

Lukowski R, Rybalkin SD, Loga F, Leiss V, Beavo JA and Hofmann F (2010) Cardiac hypertrophy is not amplified by deletion of cGMP-dependent protein kinase I in cardiomyocytes. *Proceedings of the National Academy of Sciences of the United States of America* **107**:5646-5651.

Lukowski R, Weinmeister P, Bernhard D, Feil S, Gotthardt M, Herz J, Massberg S, Zernecke A, Weber C, Hofmann F and Feil R (2008) Role of smooth muscle cGMP/cGKI signaling in murine vascular restenosis. *Arteriosclerosis, thrombosis, and vascular biology* **28**:1244-1250.

Masuyama H, Tsuruda T, Kato J, Imamura T, Asada Y, Stasch JP, Kitamura K and Eto T (2006) Soluble guanylate cyclase stimulation on cardiovascular remodeling in angiotensin II-induced hypertensive rats. *Hypertension* **48**:972-978.

McMurray JJ, Adamopoulos S, Anker SD, Auricchio A, Bohm M, Dickstein K, Falk V, Filippatos G, Fonseca C, Gomez-Sanchez MA, Jaarsma T, Kober L, Lip GY, Maggioni AP, Parkhomenko A, Pieske BM, Popescu BA, Ronnevik PK, Rutten FH, Schwitter J, Seferovic P, Stepinska J, Trindade PT, Voors AA, Zannad F, Zeiher A and Guidelines ESCCfP (2012) ESC Guidelines for the diagnosis and treatment of acute and chronic heart failure 2012: The Task Force for the Diagnosis and Treatment of Acute and Chronic Heart Failure 2012 of the European Society of

Cardiology. Developed in collaboration with the Heart Failure Association (HFA) of the ESC. *European heart journal* **33**:1787-1847.

McMurray JJ, Packer M, Desai AS, Gong J, Lefkowitz MP, Rizkala AR, Rouleau JL, Shi VC, Solomon SD, Swedberg K, Zile MR, the P-HFI and Committees (2014) Angiotensin-Neprilysin Inhibition versus Enalapril in Heart Failure. *The New England journal of medicine.*

Methner C, Lukowski R, Grube K, Loga F, Smith RA, Murphy MP, Hofmann F and Krieg T (2013) Protection through postconditioning or a mitochondria-targeted S-nitrosothiol is unaffected by cardiomyocyte-selective ablation of protein kinase G. *Basic research in cardiology* **108**:337.

Miller CL, Oikawa M, Cai Y, Wojtovich AP, Nagel DJ, Xu X, Xu H, Florio V, Rybalkin SD, Beavo JA, Chen YF, Li JD, Blaxall BC, Abe J and Yan C (2009) Role of Ca2+/calmodulin-stimulated cyclic nucleotide phosphodiesterase 1 in mediating cardiomyocyte hypertrophy. *Circulation research* **105**:956-964.

Mokni W, Keravis T, Etienne-Selloum N, Walter A, Kane MO, Schini-Kerth VB and Lugnier C (2010) Concerted regulation of cGMP and cAMP phosphodiesterases in early cardiac hypertrophy induced by angiotensin II. *PloS one* **5**:e14227.

Nagayama T, Hsu S, Zhang M, Koitabashi N, Bedja D, Gabrielson KL, Takimoto E and Kass DA (2009) Pressure-overload magnitude-dependence of the anti-hypertrophic efficacy of PDE5A inhibition. *Journal of molecular and cellular cardiology* **46**:560-567.

Nishida M, Watanabe K, Sato Y, Nakaya M, Kitajima N, Ide T, Inoue R and Kurose H (2010) Phosphorylation of TRPC6 channels at Thr69 is required for anti-hypertrophic effects of phosphodiesterase 5 inhibition. *The Journal of biological chemistry* **285**:13244-13253.

Nishikimi T, Maeda N and Matsuoka H (2006) The role of natriuretic peptides in cardioprotection. *Cardiovascular research* **69**:318-328.

Ockaili R, Salloum F, Hawkins J and Kukreja RC (2002) Sildenafil (Viagra) induces powerful cardioprotective effect via opening of mitochondrial K(ATP) channels in rabbits. *American journal of physiology Heart and circulatory physiology* **283**:H1263-1269.

Paradis P, Dali-Youcef N, Paradis FW, Thibault G and Nemer M (2000) Overexpression of angiotensin II type I receptor in cardiomyocytes induces cardiac hypertrophy and remodeling. *Proceedings of the National Academy of Sciences of the United States of America* **97**:931-936.

Patrucco E, Domes K, Sbroggio M, Blaich A, Schlossmann J, Desch M, Rybalkin SD, Beavo JA, Lukowski R and Hofmann F (2014) Roles of cGMP-dependent protein kinase I (cGKI) and PDE5 in the regulation of Ang II-induced cardiac hypertrophy and fibrosis. *Proceedings of the National Academy of Sciences of the United States of America* **111**:12925-12929.

Redfield MM, Chen HH, Borlaug BA, Semigran MJ, Lee KL, Lewis G, LeWinter MM, Rouleau JL, Bull DA, Mann DL, Deswal A, Stevenson LW, Givertz MM, Ofili EO, O'Connor CM, Felker GM, Goldsmith SR, Bart BA, McNulty SE, Ibarra JC, Lin G, Oh JK, Patel MR, Kim RJ, Tracy RP, Velazquez EJ, Anstrom KJ, Hernandez AF, Mascette AM, Braunwald E and Trial R (2013) Effect of phosphodiesterase-5 inhibition on exercise capacity and clinical status in heart failure with preserved ejection fraction: a randomized clinical trial. *Jama* **309**:1268-1277.

Rivard K, Grandy SA, Douillette A, Paradis P, Nemer M, Allen BG and Fiset C (2011) Overexpression of type 1 angiotensin II receptors impairs excitation-contraction coupling in the mouse heart. *American journal of physiology Heart and circulatory physiology* **301**:H2018-2027.

Salloum FN, Abbate A, Das A, Houser JE, Mudrick CA, Qureshi IZ, Hoke NN, Roy SK, Brown WR, Prabhakar S and Kukreja RC (2008) Sildenafil (Viagra) attenuates ischemic cardiomyopathy and improves left ventricular function in mice. *American journal of physiology Heart and circulatory physiology* **294**:H1398-1406.

Sasaki H, Nagayama T, Blanton RM, Seo K, Zhang M, Zhu G, Lee DI, Bedja D, Hsu S, Tsukamoto O, Takashima S, Kitakaze M, Mendelsohn ME, Karas RH, Kass DA and Takimoto E (2014) PDE5 inhibitor efficacy is estrogen dependent in female heart disease. *The Journal of clinical investigation* **124**:2464-2471.

Schafer S, Ellinghaus P, Janssen W, Kramer F, Lustig K, Milting H, Kast R and Klein M (2009) Chronic inhibition of phosphodiesterase 5 does not prevent pressure-overload-induced right-ventricular remodelling. *Cardiovascular research* **82**:30-39.

Soltysinska E, Bentzen BH, Barthmes M, Hattel H, Thrush AB, Harper ME, Qvortrup K, Larsen FJ, Schiffer TA, Losa-Reyna J, Straubinger J, Kniess A, Thomsen MB, Bruggemann A, Fenske S, Biel M, Ruth P, Wahl-Schott C, Boushel RC, Olesen SP and Lukowski R (2014) KCNMA1 encoded cardiac BK channels afford protection against ischemia-reperfusion injury. *PloS one* **9**:e103402.

Takeda N, Manabe I, Uchino Y, Eguchi K, Matsumoto S, Nishimura S, Shindo T, Sano M, Otsu K, Snider P, Conway SJ and Nagai R (2010) Cardiac fibroblasts are essential for the adaptive response of the murine heart to pressure overload. *The Journal of clinical investigation* **120**:254-265.

Takimoto E (2012) Cyclic GMP-dependent signaling in cardiac myocytes. *Circulation journal : official journal of the Japanese Circulation Society* **76**:1819-1825.

Takimoto E, Champion HC, Li M, Belardi D, Ren S, Rodriguez ER, Bedja D, Gabrielson KL, Wang Y and Kass DA (2005) Chronic inhibition of cyclic GMP phosphodiesterase 5A prevents and reverses cardiac hypertrophy. *Nature medicine* **11**:214-222.

Takimoto E, Koitabashi N, Hsu S, Ketner EA, Zhang M, Nagayama T, Bedja D, Gabrielson KL, Blanton R, Siderovski DP, Mendelsohn ME and Kass DA (2009) Regulator of G protein signaling 2 mediates cardiac compensation to pressure overload and antihypertrophic effects of PDE5 inhibition in mice. *The Journal of clinical investigation* **119**:408-420.

Tirziu D, Giordano FJ and Simons M (2010) Cell communications in the heart. *Circulation* **122**:928-937.

Tokudome T, Kishimoto I, Horio T, Arai Y, Schwenke DO, Hino J, Okano I, Kawano Y, Kohno M, Miyazato M, Nakao K and Kangawa K (2008) Regulator of G-protein signaling subtype 4 mediates antihypertrophic effect of locally secreted natriuretic peptides in the heart. *Circulation* **117**:2329-2339.

Vandeput F, Wolda SL, Krall J, Hambleton R, Uher L, McCaw KN, Radwanski PB, Florio V and Movsesian MA (2007) Cyclic nucleotide phosphodiesterase PDE1C1 in human cardiac myocytes. *The Journal of biological chemistry* **282**:32749-32757.

Westermann D, Becher PM, Lindner D, Savvatis K, Xia Y, Frohlich M, Hoffmann S, Schultheiss HP and Tschope C (2012) Selective PDE5A inhibition with sildenafil rescues left ventricular dysfunction, inflammatory immune response and cardiac remodeling in angiotensin II-induced heart failure in vivo. *Basic research in cardiology* **107**:308.

Xie YP, Chen B, Sanders P, Guo A, Li Y, Zimmerman K, Wang LC, Weiss RM, Grumbach IM, Anderson ME and Song LS (2012) Sildenafil prevents and reverses transverse-tubule remodeling and Ca(2+) handling dysfunction in right ventricle failure induced by pulmonary artery hypertension. *Hypertension* **59**:355-362.

Yasuda N, Akazawa H, Ito K, Shimizu I, Kudo-Sakamoto Y, Yabumoto C, Yano M, Yamamoto R, Ozasa Y, Minamino T, Naito AT, Oka T, Shiojima I, Tamura K, Umemura S, Paradis P, Nemer M and Komuro I (2012) Agonist-independent constitutive activity of angiotensin II receptor promotes cardiac remodeling in mice. *Hypertension* **59**:627-633.

Zhang M, Takimoto E, Hsu S, Lee DI, Nagayama T, Danner T, Koitabashi N, Barth AS, Bedja D, Gabrielson KL, Wang Y and Kass DA (2010) Myocardial remodeling is controlled by myocyte-targeted gene regulation of phosphodiesterase type 5. *Journal of the American College of Cardiology* **56**:2021-2030.

Footnotes

a.) This work was supported by the Deutsche Forschungsgemeinschaft (DFG) Research Unit 2060 “cGMP signalling in cell growth and survival" with grants to R.L., A.F. and V.O.N. and by the Elite Programme financed by the Landesstiftung Baden-Württemberg (to R.L.). The DFG funded Klinische Forschergruppe (KFO274) contributed to parts of the study.

Legend for Figures

Figure 1: FRET-based cGMP measurements in WT and αMHC-$AT_1R^{tg/+}$ myocytes

(A) Freshly isolated CMs from double-transgenic mice expressing AT_1R and cGMP sensor (red cGES-DE5) and littermate controls (CTR) expressing the sensor alone were treated with 1 µM CNP and the intensities of Sapphire (GFP) and Dimer2 (RFP) were measured over time. Increase in FRET ratio (GFP/RFP) corresponds to an increase in cGMP. **(B)** Quantifications of FRET ratio (means±SEM) recorded from CNP stimulated double-transgenic mice and control animals (*P<0.05; n.s.=non-significant). In additions, cells of both genotypes were treated with a combination of CNP and 100 µM IBMX to compare maximally stimulated cGMP levels under PDE inhibition. **(C)** CM from double-transgenic mice and red cGES-DE5 controls were treated with 100 µM IBMX alone and FRET ratio was calculated. **(D)** Quantifications of FRET data recorded from IBMX-treated double-transgenic mice and control cells from red cGES-DE5 positive age- and littermates (**P<0.01).

Figure 2: Role of sildenafil and cGMP/cGKI for the cardiac stress response in αMHC-$AT_1R^{tg/+}$ hearts

(A) Representative Western Blot analysis of cGKI in total protein lysates obtained from 160 **(B)** and 120 days old WT hearts and age-matched αMHC-$AT1R^{tg/+}$ litters using antibodies that specifically detect the cGKI common protein (Geiselhoringer et al., 2004; Lukowski et al., 2010). Glyceraldehyde-3-phosphate dehydrogenase (GAPDH) served as loading control. The size of the proteins was estimated by the use of a protein molecular weight standard (M_w). **(C)** Associated densitometry analysis of the cGKI abundance in total heart lysates normalized to GAPDH expression at an age of 160 and **(D)** 120 days (***P<0.001). **(E)** Global levels of cardiac cGMP were significantly higher in AT_1R transgenic hearts. cGMP values were corrected for the wet weight of the hearts (*P<0.05). **(F)** Rationale for the design of the sildenafil treatment study. **(G)** Design of the sildenafil treatment protocol. αMHC-$AT1R^{tg/+}$ and age-matched WT litters at an age of 60 days received either (a.) sildenafil (400 mg/l) in their drinking water or (b.) placebo. To test whether the progressive cardiac phenotype induced by amplified AT_1R signaling in the cardiomyocyte would be sensitive to sildenafil we adopted a previously established long-term protocol using losartan (Paradis et al., 2000).

Figure 3: Effect of sildenafil on different growth parameters of the cardiac remodeling process in αMHC-AT$_1$R$^{tg/+}$ mice

(A) The weights of the hearts were normalized to the body-weight or **(B)** to the length of the tibia in the different treatment groups (placebo or sildenafil) and genotypes (WT and αMHC-AT1R$^{tg/+}$). 60-days of sildenafil (SIL) did not change the progressive cardiac growth phenotype of αMHC-AT1R$^{tg/+}$ mice (number signs (#) and section signs (§) indicate statistical difference between the two genotypes -SIL (#) or +SIL (§) yielding p-values of $^{###/§§§}$P<0.001; n.s.=non-significant). Note, the basal values from Fig. 1A (120 days) were implemented in this panel. Quantitative analyses of transcript levels of the cardiac hypertrophy markers **(C)** atrial natriuretic peptide (ANP), **(D)** brain natriuretic peptide (BNP), **(E)** myosin heavy chain α-isoform (αMHC), and **(F)** cardiac sarcoplasmatic reticulum Ca^{2+}-ATPase-2 (SERCA2) in hearts obtained from 120 days old WT and αMHC-AT1R$^{tg/+}$ mice that received either SIL (400 mg/l for 60 days) or remained untreated. Hypoxanthine-phosphoribosyl-transferase 1 (HPRT1) mRNA levels were used as a reference to normalize the data (number signs (#) and section signs (§) indicate statistical difference between the two genotypes -SIL (#) or +SIL (§) yielding p-values of §P<0.05 for ANP, $^{#}$P<0.05 and §§§P<0.001 for BNP, and $^{##}$P<0.01 for SERCA2). **(G)** Representative hematoxylin and eosin staining of cardiac sections from sildenafil treated and control αMHC-AT1R$^{tg/+}$ mouse hearts. **(H)** The histological sections shown in (G) were used to determine the cross-section areas of cardiomyocytes from αMHC-AT1R$^{tg/+}$ hearts ±sildenafil. In total 438 and 480 cells from untreated and sildenafil treated αMHC-AT1R$^{tg/+}$ mice, respectively were quantified as described in the method section. Sildenafil treatment did not reduce the area of the myocytes. cGMP values were determined in **(I)** total hearts and **(J)** aorta from αMHC-AT$_1$R$^{tg/+}$ mice that were either treated with SIL (400 mg/l) in their drinking water for 7 days or remained untreated. All measurements were corrected for the wet-weight of the tissue samples (*P<0.05). Numbers are indicative for the tissue samples that were analyzed. Note, the raise in total cardiac cGMP levels just met the statistical significance (P=0.05), whereas the effect of the drug on the aorta was more pronounced.

Figure 4: Analysis of the fibrotic response in αMHC-AT1R$^{tg/+}$ mice ±sildenafil for 60 days

(A) Sirius Red staining of cardiac sections was performed to visualize interstitial fibrosis *i.e.* collagen fibers in WT and αMHC-AT1R$^{tg/+}$ hearts obtained from mice that either received sildenafil (400 mg/l) or remained untreated. **(B)** Quantification of the amount of fibrosis using GSA Imager software package on sections from n=6 to 9 mice per genotype. Fibrosis is represented by the red color shown in (A) and was referred to the total size of the heart muscles in different genotypes and groups (number signs (#) and section signs (§) indicate statistical difference between the two genotypes -SIL (#) or +SIL (§) yielding p-values of $^{\#\#\#/\S\S\S}P<0.001$; n.s.=non-significant). HPRT1 normalized expression levels of fibrosis marker genes and extracellular matrix turn-over regulating genes were quantified using specific RT-PCR primer-pairs for **(C)** collagen alpha-1 chain-1 (Col1A1), **(D)** collagen alpha-1 chain-2 (Col1A2), **(E)** matrix metalloproteinase-9 (MMP9), and **(F)** metallopeptidase inhibitor-1 (TIMP1) (section signs (§) indicate statistical difference between the two genotypes +SIL yielding a p-value of $^{\S}P<0.05$ for MMP9 and TIMP1).

Figure 5: Effects of sildenafil on distorted cardiac functions of αMHC-AT1R$^{tg/+}$ mice and the expression levels of different cGMP-hydrolyzing PDEs

(A) Representative cardiac geometries such as the LV end-systolic diameter (LVESD) and LV end-diastolic diameter (LVEDD) were determined by echocardiography in M-mode traces of WT and αMHC-AT1R$^{tg/+}$ hearts. **(B)** Fractional shortening (%FS) and **(C)** percent ejection fraction (%EF) were measured from M-mode images and averaged over nine measurements per mouse. Sildenafil did not attenuate the functional decline induced by the CM-specific over-expression of the AT_1R (number signs (#) and section signs (§) indicate statistical difference between the two genotypes -SIL (#) or +SIL (§) yielding p-values of $^{\#\#\#/\S\S\S}P<0.001$ for %FS and EF; n.s.=non-significant). No significant changes were detectable for the expression levels of the cGMP-hydrolyzing **(D)** phosphodiesterase 5 (PDE5) between the control and sildenafil treated mice. **(E)** Cardiac cGMP hydrolyzing activity was determined in the presence of EGTA or **(F)** Ca^{2+}/CaM using 1 µM of ^{32P}-cGMP as a substrate. All dose-response curves were determined from normal WT (n=12) and hypertrophic αMHC-$AT_1R^{tg/+}$

(n=13) heart lysates upon acutely adding SIL (0.1 to 1000 nM). Cyclic GMP-hydrolyzing activities were not significantly different between the two genotypes at all conditions tested. If anything we observed a tendency for a different cGMP-hydrolyzing activity (1 to 100 nM of SIL) in (E).

Table 1: *In vivo effects of sildenafil in different rodent models of right/left cardiac hypertrophy and fibrosis*

Model	Species	Sildenafil protocol	Therapeutic effect(s) of the drug		Reference(s)
			HW[6] and/or cardiomyocyte hypertrophy	Quantitative markers of fibrosis	
TAC[1]	mouse	100 mg·kg^{-1}·d^{-1} in rodent chow	↓	↓	(Takimoto et al., 2005)
PAB[2]	rat	100 mg·kg^{-1}·d^{-1} in drinking water	no effect	no effect	(Andersen et al., 2008)
PAB[2]	rat	50 mg·kg^{-1}·d^{-1} in drinking water	↑	↑	(Schafer et al., 2009)
Monocrotaline injection	rat	50 mg·kg^{-1}·d^{-1} in drinking water	↓	↓	(Schafer et al., 2009)
sTAC[3]	mouse	200 mg·kg^{-1}·d^{-1} in rodent chow	↓	not reported	(Nagayama et al., 2009)
mTAC[4]	mouse	200 mg·kg^{-1}·d^{-1} in rodent chow	no effect	not reported	(Nagayama et al., 2009)
TAC[1]	mouse	200 mg·kg^{-1}·d^{-1} in rodent chow	↓	not reported	(Blanton et al., 2012)
Ang II infusion	mouse	400 mg/l in drinking water	no effect	↓	(Patrucco et al., 2014)
Ang II infusion	mouse	100 mg·kg^{-1}·d^{-1} in rodent chow	↓	↓	(Westermann et al., 2012)
PAB[2]	rat	100 mg·kg^{-1}·d^{-1} in drinking water	no effect	↓	(Borgdorff et al., 2014)
TAC[1]	OVX[5] mouse	100 mg·kg^{-1}·d^{-1} in rodent chow	no effect	not reported	(Sasaki et al., 2014)
TAC[1]	mouse	200 mg·kg^{-1}·d^{-1} in rodent chow	no effect	↓	(Lee et al., 2015)
CM-restricted AT_1R overexpression	mouse	400 mg/l in drinking water	no effect	no effect	(Straubinger et al., this study)

[1]Transverse aortic constriction; [2]pulmonary aortic banding; [3]severe transverse aortic constriction (3 weeks); [4]moderate transverse aortic constriction (3 weeks) [5]ovariectomy; [6]heart weight

Fig. 1

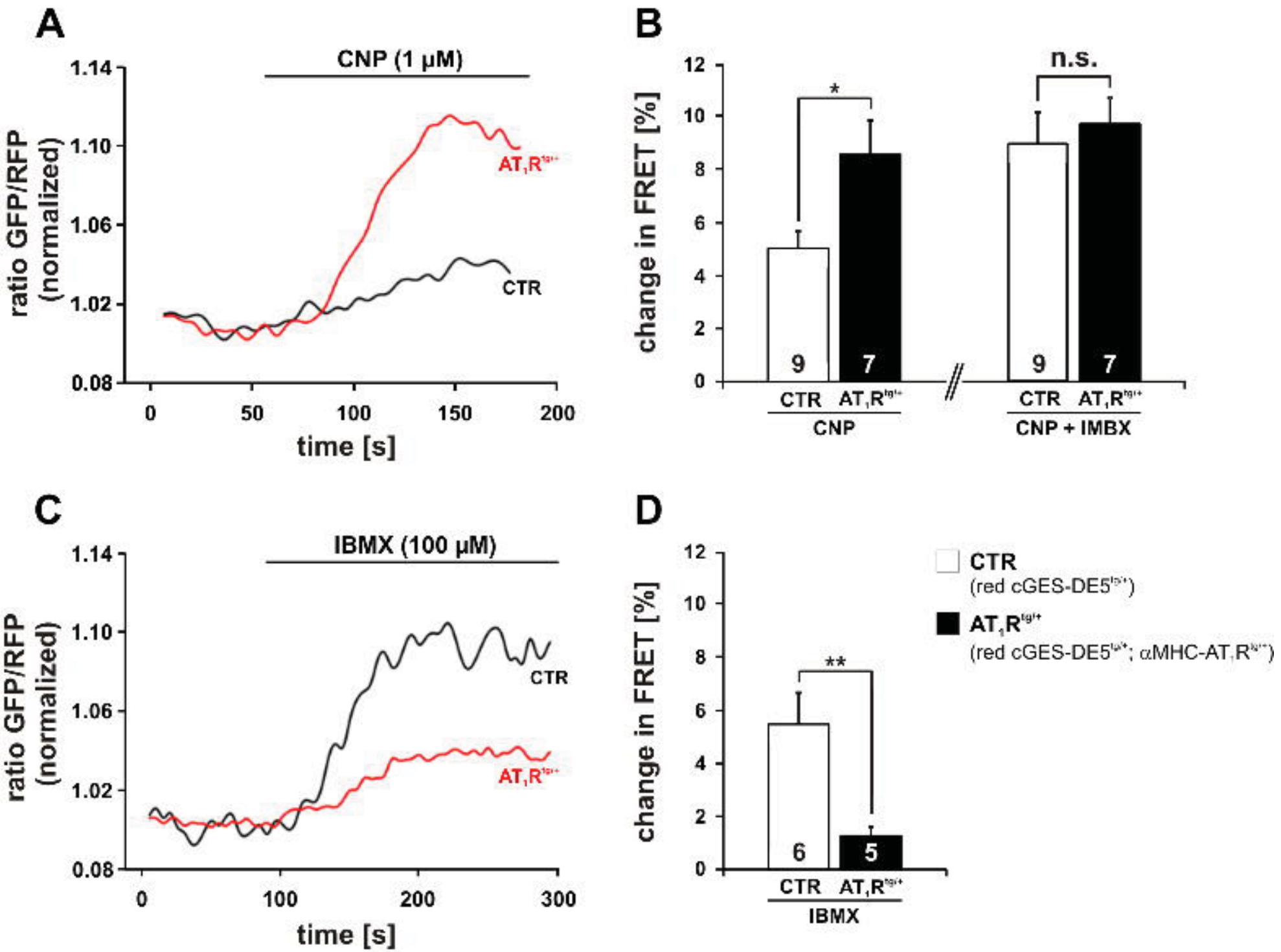
A
CNP (1 µM)
ratio GFP/RFP (normalized)
1.14
1.10
1.06
1.02
0.08
0
50
100
150
200
time [s]
AT1R tg/+
CTR
B
change in FRET [%]
12
10
8
6
4
2
0
*
n.s.
9
7
9
7
CTR
AT1R tg/+
CTR
AT1R tg/+
CNP
CNP + IMBX
C
IBMX (100 µM)
ratio GFP/RFP (normalized)
1.14
1.10
1.06
1.02
0.08
0
100
200
300
time [s]
CTR
AT1R tg/+
D
change in FRET [%]
12
10
8
6
4
2
0
**
6
5
CTR
AT1R tg/+
IBMX
CTR
(red cGES-DE5 tg/+)
AT1R tg/+
(red cGES-DE5 tg/+; αMHC-AT1R tg/+)

Fig. 2

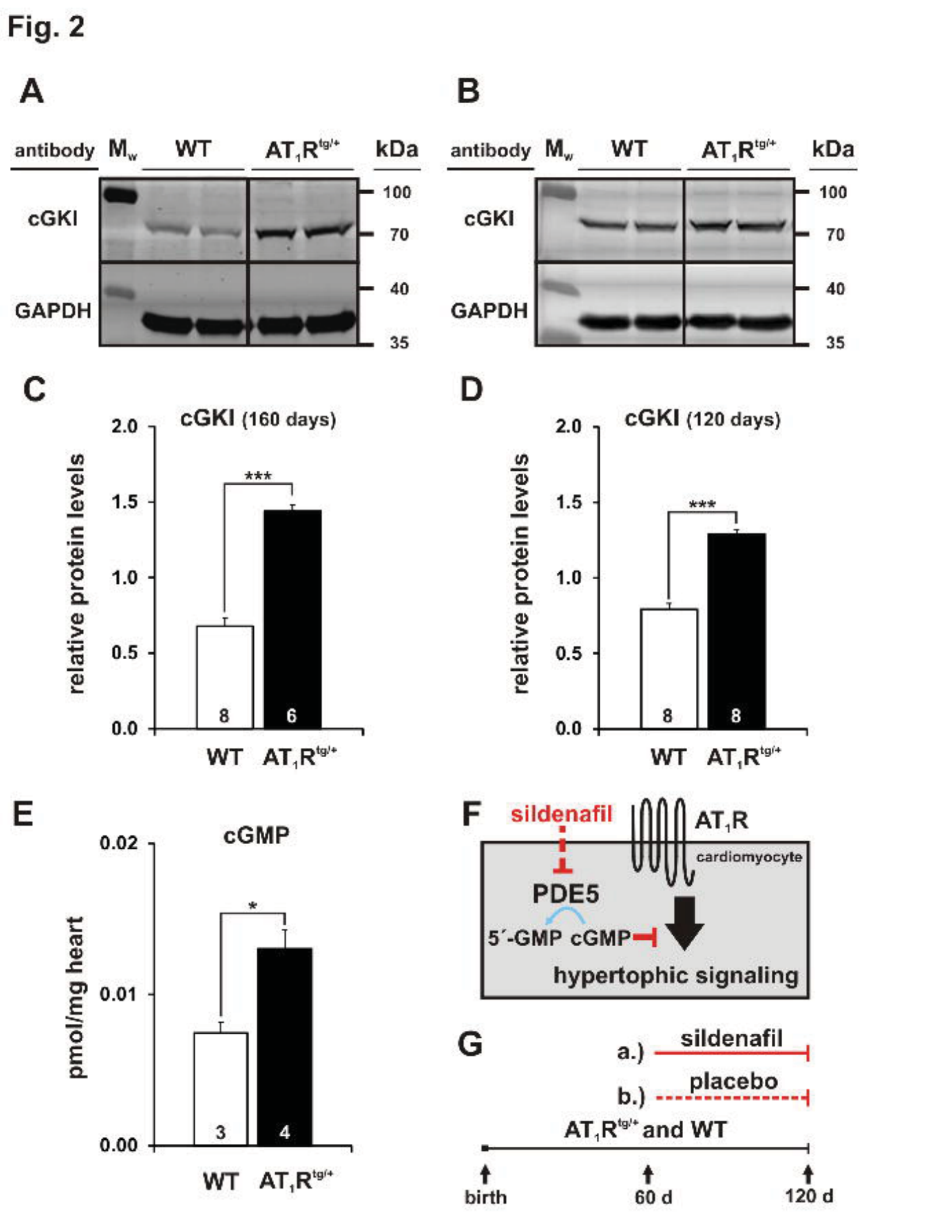
A
antibody
Mw
WT
AT1Rtg/+
kDa
cGKI
GAPDH
100
70
40
35
B
antibody
Mw
WT
AT1Rtg/+
kDa
cGKI
GAPDH
100
70
40
35
C
cGKI (160 days)
relative protein levels
2.0
1.5
1.0
0.5
0.0
***
8
6
WT
AT1Rtg/+
D
cGKI (120 days)
relative protein levels
2.0
1.5
1.0
0.5
0.0
***
8
8
WT
AT1Rtg/+
E
cGMP
pmol/mg heart
0.02
0.01
0.00
*
3
4
WT
AT1Rtg/+
F
sildenafil
AT1R
cardiomyocyte
PDE5
5´-GMP
cGMP
hypertophic signaling
G
a.) sildenafil
b.) placebo
AT1Rtg/+ and WT
birth
60 d
120 d

Fig. 3

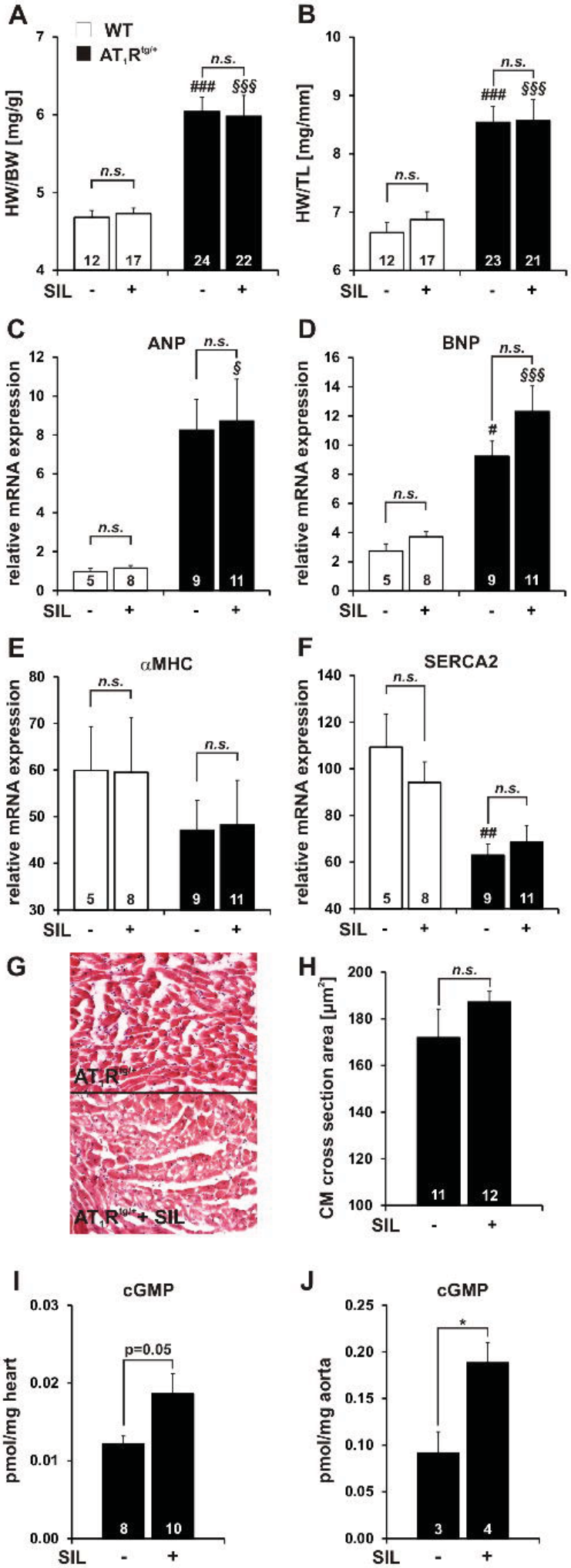
A
WT
AT1R tg/+
HW/BW [mg/g]
n.s.
###
§§§
n.s.
12
17
24
22
SIL - + - +
B
HW/TL [mg/mm]
n.s.
###
§§§
n.s.
12
17
23
21
SIL - + - +
C
ANP
relative mRNA expression
n.s.
§
n.s.
5
8
9
11
SIL - + - +
D
BNP
relative mRNA expression
n.s.
§§§
#
n.s.
5
8
9
11
SIL - + - +
E
αMHC
relative mRNA expression
n.s.
n.s.
5
8
9
11
SIL - + - +
F
SERCA2
relative mRNA expression
n.s.
n.s.
##
5
8
9
11
SIL - + - +
G
AT1R tg/+
AT1R tg/+ + SIL
H
CM cross section area [µm²]
n.s.
11
12
SIL - +
I
cGMP
pmol/mg heart
p=0.05
8
10
SIL - +
J
cGMP
pmol/mg aorta
*
3
4
SIL - +

Fig. 4

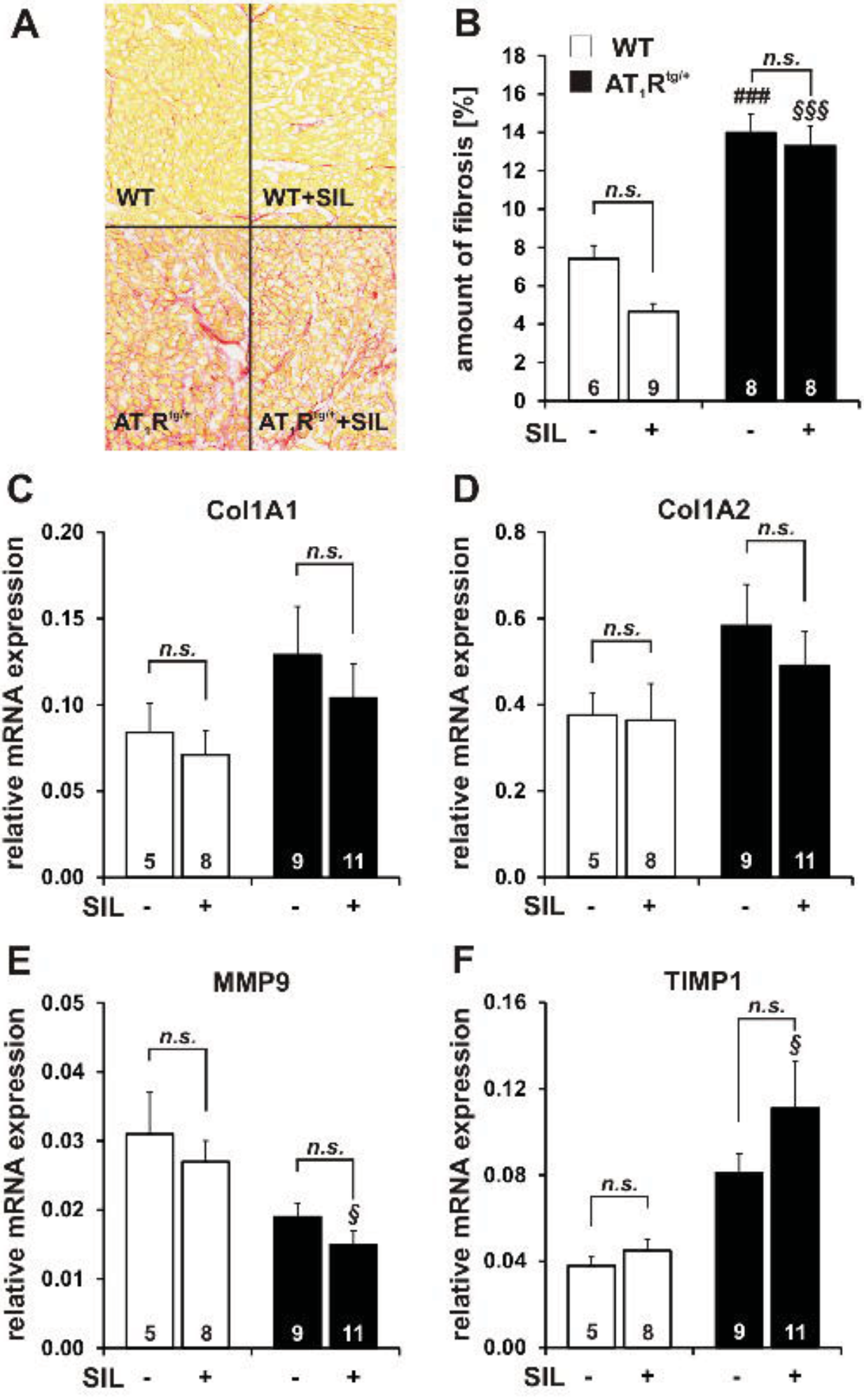
A
WT
WT+SIL
AT1R tg/+
AT1R tg/+ +SIL
B
WT
AT1R tg/+
amount of fibrosis [%]
n.s.
n.s.
###
§§§
6
9
8
8
SIL - + - +
C
Col1A1
relative mRNA expression
n.s.
n.s.
5
8
9
11
SIL - + - +
D
Col1A2
relative mRNA expression
n.s.
n.s.
5
8
9
11
SIL - + - +
E
MMP9
relative mRNA expression
n.s.
n.s.
§
5
8
9
11
SIL - + - +
F
TIMP1
relative mRNA expression
n.s.
n.s.
§
5
8
9
11
SIL - + - +

Fig. 5

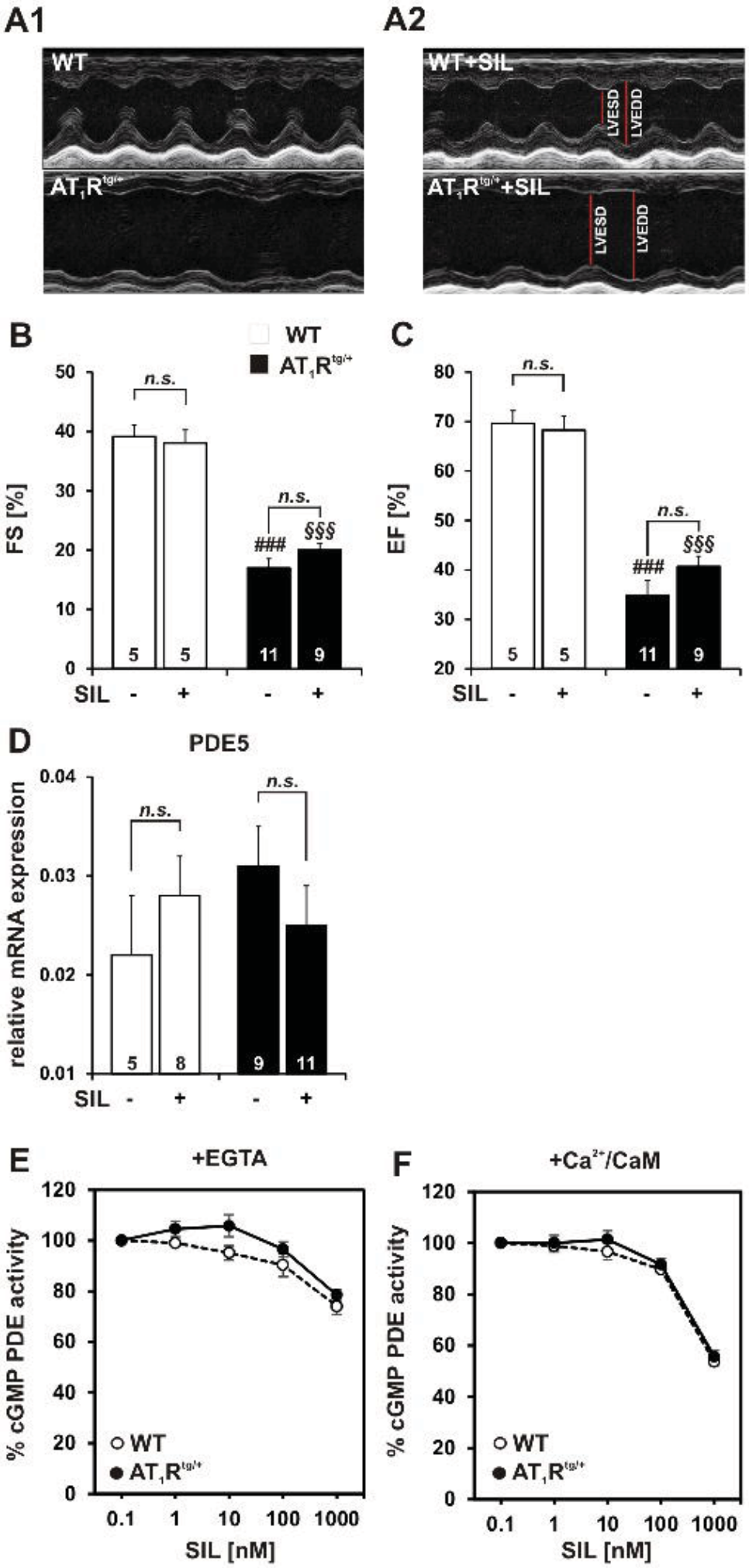
A1
A2
WT
AT1R tg/+
WT+SIL
AT1R tg/+ +SIL
LVESD
LVEDD
B
C
WT
AT1R tg/+
FS [%]
EF [%]
n.s.
###
§§§
5
11
9
SIL
D
PDE5
relative mRNA expression
8
E
+EGTA
F
+Ca2+/CaM
% cGMP PDE activity
SIL [nM]
0.1
1
10
100
1000